1*H*-Cyclopentapyrimidine-2,4(1*H*,3*H*)-dione-Related Ionotropic Glutamate Receptors Ligands. Structure−Activity Relationships and Identification of Potent and Selective iGluR5 Modulators

Stefania Butini,[¶,⊥] Darryl S. Pickering,[‡] Elena Morelli,[§,⊥] Salvatore Sanna Coccone,[¶,⊥] Francesco Trotta,[¶,⊥] Meri De Angelis,[¶,⊥] Egeria Guarino,[¶,⊥] Isabella Fiorini,[¶,⊥] Giuseppe Campiani,*[,¶,⊥] Ettore Novellino,[§,⊥] Arne Schousboe,[‡] Jeppe K. Christensen,[#] and Sandra Gemma[¶,⊥]

European Research Centre for Drug Discovery and Development (NatSynDrugs), Banchi di Sotto 55, 53100 Siena, Italy, Dipartimento Farmaco Chimico Tecnologico (DFCT), Università degli Studi di Siena, Via Aldo Moro, 53100 Siena, Italy, Dipartimento di Chimica Farmaceutica e Tossicologica (DCFT), Università di Napoli Federico II, Via D. Montesano 49, 80131 Napoli, Italy, Department of Pharmacology and Pharmacotherapy, Faculty of Pharmaceutical Sciences, University of Copenhagen, 2 Universitetsparken, DK-2100 Copenhagen, Denmark, and NeuroSearch A/S, Pederstrupvej 97, Ballerup Denmark

Received July 14, 2008

(*S*)-CPW399 ((*S*)-**1**) is a potent and excitotoxic AMPA receptor partial agonist. Modifying the cyclopentane ring of (*S*)-**1**, we developed two of the most potent and selective functional antagonists (**5** and **7**) for kainate receptor (KA-R) subunit iGluR5. Derivatives **5** and **7**, with their unique pharmacological profile, may lead to a better understanding of the different roles and modes of action of iGluR1−5 subunits, paving the way for the synthesis of new potent, subunit selective iGluR5 modulators.

Introduction

L-Glutamate (Glu) is the major excitatory neurotransmitter in the mammalian central nervous system (CNS), and it modulates the functions of most neuronal circuits in the CNS. The physiological and pathological actions of Glu are mediated by activation of a range of excitatory amino acid transporters, ionotropic glutamate receptors (iGluRs, ligand-gated ion channels), and the metabotropic glutamate receptors (mGluRs, G-protein-coupled). Binding of Glu to iGluRs, which are abundantly expressed in the brain, is a key step in the predominant mechanism of rapid excitatory synaptic transmission in the CNS. Even if the complex roles of the iGluRs are far from being understood in detail, it is generally accepted that these receptors are implicated in learning and memory formation and are associated with a number of psychiatric and neurological disorders such as Alzheimer's, Parkinson's, and Huntington's diseases, schizophrenia, amyotrophic lateral sclerosis, and epilepsy.[1] iGluRs in the mammalian brain are encoded by a family of 18 genes that coassemble to form the kainate, *N*-methyl-D-aspartate and (*S*)-2-amino-3-(5-methyl-3-hydroxyisoxazol-4-yl)propanoic acid receptors (KA-R, NMDA-R, and AMPA-R, respectively). Coassembly of these ion channel proteins within the families generates several receptor subtypes. iGluRs form tetrameric ligand-gated ion channels, and one copy of the ligand-binding core, as a discrete domain, is present in each subunit.[2]

A major focus in studying the mechanism of excitotoxicity and excitatory amino acid induced neuronal cell death has involved the role of the NMDA subtype of iGluRs because of its ability to flux large amounts of potentially lethal Ca^{2+} ions into the cell.[3] Less attention has been directed to AMPA-Rs and KA-Rs, since for many years selective agonists and antagonists were not available. The successful structural analysis of the ligand-binding cores of AMPA-R and KA-R subunits recently boosted the development of subtype selective iGluRs modulators.[4−7] It is now accepted that among the cloned AMPA and KA iGluRs, subunits iGluR1−4 are AMPA sensitive, while the KA-Rs are composed of iGluR5−7 and KA1,2 subunits. iGluR5−7 in combination with KA1 and KA2 subunits can form functional homomeric or heteromeric ion channels. KA-Rs are widely distributed in the CNS, including the dorsal horn and dorsal root ganglion (DRG) neurons. The iGluR5 subunit is the most readily detectable at presynaptic sites in the DRG. iGluRs play a principal role in spinal cord nociceptive transmission, and activation of iGluRs in central endings of DRG neurons depolarizes primary afferents and may sustain presynaptic inhibition of C fibers. Thus, presynaptic KA-Rs may play an important role in the modulation of nociception, being a novel target for therapeutic strategies. However, the role of KA-Rs in brain function is not fully understood yet; therefore, potent and highly selective agonists and antagonists are still needed.

We have previously reported the synthesis of (*S*)-CPW399 ((*S*)-**1**, Chart 1),[4] a iGluRs ligand characterized by a bicyclic scaffold and structurally related to the naturally occurring (*S*)-willardiine (**2a**). Derivative (*S*)-**1** was found to be a selective, partial agonist for iGluR1/iGluR2 subunits that, unlike (*S*)-**2a**, stimulated an increase in $[Ca^{2+}]$ in mouse cerebellar granule cells and induced neuronal cell death. Recently we provided the X-ray structure of (*S*)-**1** in complex with the ligand binding core of the iGluR2 subunit and with the (Y702F)GluR2-S1S2J mutant, enabling an understanding of the molecular mechanisms underlying the iGluR1,2 vs iGluR3,4 subtype selectivity of (*S*)-**1**.[8]

To improve the structure−activity relationships (SARs) of the class of bicyclic analogues of willardiine, typified by (*S*)-**1**, a new set of related analogues was developed on the basis of the X-ray structures of (*S*)-**1** in complex with the ligand-binding core of iGluR2 (GluR2-S1S2J) and (Y702F)GluR2-S1S2J and on the basis of the crystal structures of the iGluR5 and iGluR6 KA-R ligand binding cores in complexes with Glu (the molecular modeling studies will be reported elsewhere). A number of SAR trends was identified in the series of the bicyclic analogues of (*S*)-**1**, and two of the most potent iGluR5 selective

* To whom correspondence should be addressed. Phone: 0039-0577-234172. Fax: 0039-0577-234333. E-mail: campiani@unisi.it.
¶ Università degli Studi di Siena.
⊥ European Research Centre for Drug Discovery and Development.
‡ University of Copenhagen.
§ Università di Napoli Federico II.
# NeuroSearch A/S.

10.1021/jm800865a CCC: $40.75
Published on Web 09/24/2008

Chart 1. Reference and Title Compounds

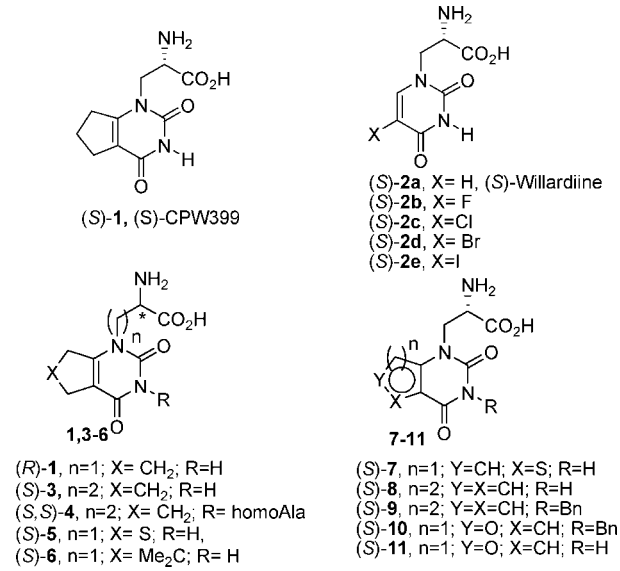

antagonists, the sulfur-bridged analogues **5** and **7**, were identified. These compounds represent novel pharmacological tools for investigation of the role of the iGluR5 subunit in neurotoxic and neurodegenerative diseases.

Results and Discussion

AMPA-R and KA-R subtype selectivity was investigated by examining the binding affinity of **1**−**8** and **11** (**9** and **10** could not be tested, being insoluble in the test conditions) at the recombinant rat AMPA-Rs (GluR1−4) and KA-Rs (GluR5,6) expressed in *Sf9* cells (Table 1); a comparison was made with (*R,S*)-AMPA, (L)-Glu, KA, (*S*)-**1**, (*R,S*)-**2a**, and its halogenated analogues (**2b**−**e**). Table 2 summarizes the potencies (EC_{50}) of willardiine analogues and compounds (*S*)-**1**, **5**, and **7** at recombinant AMPA-Rs expressed in *Xenopus laevis* oocytes.

In Vitro Pharmacology. 1. Radioligand Binding Assays. All the compounds tested can be divided into (i) derivatives having the same cyclopentyl ring of (*S*)-**1** and the pyrimidinedione portion modified or (ii) compounds in which the pyrimidinedione portion of (*S*)-**1** is preserved and modifications are introduced at the cycloalkyl-fused system. In general, all modification on the pyrimidinedione portion gave a decrease in the affinity toward all receptor subtypes; in particular, a drastic reduction was observed when a longer amino acidic chain was introduced ((*S*)-**1** vs **3**) or when a substituent is presented on N^3 position ((*S*)-**1** vs **4**). Low affinity was also observed for (*R*)-**1**, being around 100 times less active than its enantiomer counterpart. A totally different behavior was found for compounds in which changes were introduced at the cycloalkyl-fused system; in general these derivatives exhibit a broad range of affinity/selectivity, some of them binding preferably iGluR1−iGluR2 subunits, while others showing excellent affinity for the KA-R subunit iGluR5. The introduction of two methyl groups at the cyclopentyl level of (*S*)-**1** generated **6**, which was, among AMPA-R subunits, selective toward iGluR1−iGluR2. By comparison of AMPA-R versus KA-R affinity, **6** was found 22 times less active on iGluR5, indicating that **6** was endowed of significant iGluR1/iGluR2 selectivity, being 9 times more potent with respect to iGluR5. The sulfur-bridged analogues **5** and **7** were tested against AMPA-R and KA-R. At iGluR1−iGluR2 these analogues proved to be 2-fold more potent than (*S*)-**1**, with an affinity of 58 and 80 nM for **5** and 50 and 112 nM for **7** (Table 1), while on iGluR3−iGluR4 subtypes showed an affinity in the submicromolar range. When tested against KA-R subunits, iGluR5 and iGluR6 expressed in *Sf9* cells, compounds **5** and **7** showed a very high affinity. Both compounds, displaying a K_i of 5 and 5.3 nM at iGluR5, respectively, and a very weak occupancy of the iGluR6 subunit, may be considered two of the most potent and selective iGluR5 ligands known to date. They are around 8 times more potent than (*S*)-**1** and 15-fold more potent than kainate. By comparison of the affinity for subtypes iGluR1−4 and for iGluR5,6, it appears that the analogue (*S*)-**7** is a potent and selective ligand for iGluR5 KA-R subtype.

2. Electrophysiological Assays. The potencies (EC_{50}) of (*S*)-**1**, **5**, and **7** at recombinant rat AMPA-R was measured on receptors expressed in *Xenopus laevis* oocytes (Table 2). The efficacies of (*S*)-**1**, **5**, and **7** were also determined in comparison to 1 mM Glu, all in the presence of 100 μM cyclothiazide (CTZ) to block receptor desensitization. The three compounds behave as partial agonists at AMPA-Rs, and their efficacy at iGluR2$(Q)_i$ is as follows (mean ± SEM): (*S*)-**1**, 0.432 ± 0.036 ($n = 21$); **5**, 0.376 ± 0.025 ($n = 12$); **7**, 0.329 ± 0.033 ($n = 10$). These efficacy values are not statistically significantly different from one another ($P = 0.136$, one-way ANOVA). As was observed with the K_i values, **5** and **7** are more potent at iGluR1,2 than at iGluR3,4, with derivative **7** showing better selectivity for iGluR1−iGluR2 than **5**. It is noteworthy that while derivative **5** has a similar potency for all AMPA-R subtypes (EC_{50} ranging from 11 to 34 μM), **7** is about 10-fold more potent at iGluR1,2 than at iGluR3,4. This difference in selectivity between derivatives **5** and **7** at iGluR3,4 could indicate that the efficacy and/or desensitization properties of **7** at these subunits are different from those of **5**.

The pharmacology of **5** and **7** was further examined at human $iGluR1_i$ and human iGluR5$(Q)_{1b}$ expressed in the mammalian cell line CHO-K1 and using whole-cell patch-clamp electrophysiology. Both compounds were weak partial agonists at human $iGluR1_i$, and responses could only be determined in the presence of CTZ (30 μM) to block receptor desensitization (Figure 1): **5**, $EC_{50} = 18.5$ μM (95% CI, 4.3−78 μM); **7**, $EC_{50} = 4.1$ μM (95% CI, 2.3−7.3 μM). These potencies of **5** and **7** are comparable to those measured at rat $iGluR1_i$ expressed in *X. laevis* oocytes (Table 2), although the efficacies (0.16 and 0.27, respectively) are somewhat lower than those measured at rat iGluR2$(Q)_i$, indicating a species or iGluR subtype difference in desensitization. Both **5** and **7** were also very weak partial agonists at human iGluR5$(Q)_{1b}$ and exhibited rapid desensitization kinetics such that complete desensitization was obtained within 10 ms (Figure 2). Because of their high affinity, extremely slow washout, and their weak responses, EC_{50} could not be determined for **5** and **7** at iGluR5$(Q)_{1b}$. However, efficacy estimates were made using saturating concentrations of **5** and **7** with 10 mM Glu as the full agonist control ($\varepsilon = 1$): **5**, $\varepsilon = 0.12$; **7**, $\varepsilon = 0.35$ (Figure 2).

The very low efficacies of **5** and **7** at iGluR5$(Q)_{1b}$ and their rapid desensitization rates suggested that **5** and **7** could have antagonistic properties at this receptor. Indeed, both compounds were able to inhibit the responses to 3 mM Glu (Figure 3) with extremely low IC_{50} values (**5** = 3.8 nM, **7** = 1.9 nM) comparable to their affinities at rat iGluR5$(Q)_{1b}$ measured by radioligand binding (Table 1). Glu responses (1 mM) at $iGluR1_i$ were also antagonized by higher concentrations of **7** ($IC_{50} =$ 374 nM; 95% CI, 316−444 nM)), in keeping with its partial agonist nature (Figure 3).

Table 1. Binding Affinities at Recombinant Rat AMPA-R and KA-R Expressed in *Sf9* Cells

	K_i (nM)[a]					
compd	iGluR1$_o$	iGluR2$_o$(*R*)	iGluR3$_o$	iGluR4$_o$	iGluR5(*Q*)$_{1b}$	iGluR6 (*V*, *C*, *R*)
(*R*,*S*)-AMPA	21.9 ± 4.4	16.8 ± 2.9	20.6 ± 2.6	40 ± 20	1150 ± 114	NA
L-Glu	169 ± 27	282 ± 90	249 ± 12	354 ± 178	140 ± 7	332 ± 21
kainate	477 ± 76	3690 ± 980	1980 ± 340	3570 ± 700	76 ± 27	12.7 ± 3.5
(*S*)-**1**	109 ± 5	223 ± 24	1890 ± 580	2090 ± 495[b]	44 ± 7	NA
(*R*,*S*)-**2a**	410 ± 55	1220 ± 305	19000 ± 480	14200 ± 3500	>100000	NA
(*S*)-**2b**	2.9 ± 1.6	4.0 ± 2.7	70 ± 8	123 ± 12	1380 ± 137	>100000
(*S*)-**2c**[b]	37 ± 2	45 ± 6	451 ± 163	561 ± 105	47 ± 19	>100000
(*R*,*S*)-**2d**	35 ± 5	61 ± 3	434 ± 97	656 ± 48	14.8 ± 2.2	>100000
(*S*)-**2e**	83 ± 8	105 ± 27	976 ± 287	738 ± 115	2.4 ± 0.2	>100000
(*R*)-**1**	10400 ± 4250	17800 ± 7350	>100000	>100000	NT	NT
(*S*)-**3**	>100000	>100000	>100000	>100000	NA	NA
(*S*,*S*)-**4**	>100000	>100000	>100000	>100000	NA	>100000
(*S*)-**5**	58 ± 18	80 ± 30	311 ± 22	288 ± 124	5.2 ± 0.5	NA
(*S*)-**6**	102 ± 30	126 ± 8	1510 ± 570	1590 ± 590	976 ± 470	NA
(*S*)-**7**	50 ± 7	112 ± 26	936 ± 114	804 ± 38	5.3 ± 1.3	NA
(*S*)-**8**	2390 ± 172	3390 ± 496	6910 ± 663	15700 ± 7400	490 ± 110	NA
(*S*)-**11**	35200 ± 10200	43600 ± 8800	>100000	>100000	2980 ± 1050	NA

[a] Mean values ± SD from at least three experiments conducted in triplicate. NT = not tested. NA = not active (K_i > 1 mM). [b] Pooled values from iGluR4$_o$ and iGluR4c$_o$.

Table 2. Potencies (EC_{50}) of Willardiine Analogues and Compounds **1**, **6**, and **8** at Recombinant AMPA-Rs Expressed in *Xenopus lævis* Oocytes

	EC_{50} (μM)[a]			
compd	iGluR1	iGluR2(*Q*)	iGluR3	iGluR4
(*S*)-willardiine (**2a**)[b,e]	11.5 ± 1.8	NT	NT	NT
(*S*)-**2b**[c,f]	0.38 ± 0.07 (6)	0.46 ± 0.04 (10)	20.9 ± 1.9 (8)	11.9 ± 1.8 (5)
(*S*)-**2c**[f]	NT	2.11 ± 0.20 (8)	NT	NT
(*S*)-**2d**[b,e]	2.8 ± 0.4	NT	NT	NT
(*S*)-**2e**[b,e]	33.6 ± 6.5	NT	NT	NT
(*S*)-(**1**)[d,e]	24.9 ± 3.6	13.9 ± 1.4	224 ± 20	34.3 ± 2.1[g]
(*S*)-**5**[f]	11.8 ± 1.6 (8)	12.6 ± 0.6 (6)	33.9 ± 3.4 (8)[i]	24.2 ± 2.4 (10)[i]
(*S*)-**7**[f]	7.2 ± 0.8 (6)[h]	11.8 ± 1.1 (5)[h]	120 ± 14 (9)[i]	90 ± 15 (14)[i]

[a] Values are the mean ± SEM. Number of oocytes *N* in parentheses. *N* = 3−5 for compound (*S*)-**1**. NT = not tested. [b] From ref 10 (mean ± SD). [c] From ref 11. [d] From ref 4. [e] EC_{50} at flop receptors. [f] EC_{50} at flip receptors. [g] EC_{50} at iGluR4c$_o$. [h] Statistically significantly different from EC_{50} at iGluR3 and iGluR4 (P < 0.05, one-way ANOVA with Bonferroni t test). [i] Statistically significantly different (P < 0.05, one-way ANOVA with Bonferroni t test).

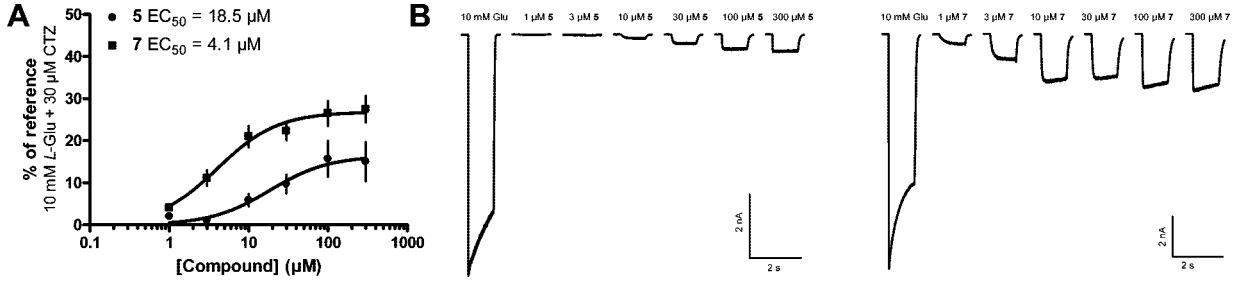

Figure 1. **5** and **7** activate human iGluR1$_i$ expressed in CHO-K1 cells. (A) Dose−response curves for the activation of iGluR1$_i$ by **5** (filled circles, EC_{50} = 18.5 μM) and **7** (filled squares, EC_{50} = 4.1 μM) in the presence of 30 μM CTZ. Values were normalized to a maximal current induced by 10 mM L-Glu in the presence of 30 μM CTZ and represent the mean ± SEM of 3–4 separate experiments. (B) Representative current responses induced by **5** (left) and **7** (right) in a iGluR1$_i$ expressing cell, which was voltage-clamped at −60 mV in the whole-cell configuration. The stimulations were conducted in the presence of 30 μM CTZ. The cell was initially subjected to 1 s pulses of 10 mM L-Glu. After the washout of L-Glu, increasing concentrations of **5** and **7** were applied to the cell in 1 s pulses.

N^3-Substituted willardiine analogues have also been shown to be antagonists at iGluR5, some having nanomolar affinity and iGluR5 selectivity.[9] However, no agonist activity was reported for these compounds, suggesting that, unlike the bicyclic compounds described herein, they are full antagonists. Additionally, the binding mode at iGluR5 of one of the most potent N^3-substituted analogues was experimentally determined. While the binding mode of our lead compound (*S*)-**1** was determined at iGluR2,[8] it has not been experimentally evaluated at iGluR5. X-ray determination of **5** in complex with the binding core of iGluR5 subunit is in progress. Given the differences in the structures of the two series of compounds, it would seem unlikely that they bind to iGluR5 in the same fashion. It could therefore be speculated that bicyclic N^3-substituted willardiine analogues could bind to iGluR5 with even higher affinity than the currently existing antagonists.

Conclusion

In summary, we prepared novel ligands for AMPA-R and KA-R structurally related to the bicyclic willardiine analogue (*S*)-**1**. Analysis of the X-ray structure of (*S*)-**1** in complex with GluR2-S1S2J and with a (Y702F)GluR2-S1S2J mutant allowed the development of derivative **6** endowed with improved selectivity for iGluR1−iGluR2 subunits. Furthermore, through a structural modification of the cyclopentane ring of (*S*)-**1**, we developed two of the most potent and selective functional antagonists (**5** and **6**) for KA-R subunit iGluR5. Derivatives **5** and **6**, with their unique pharmacological profile, may lead to a

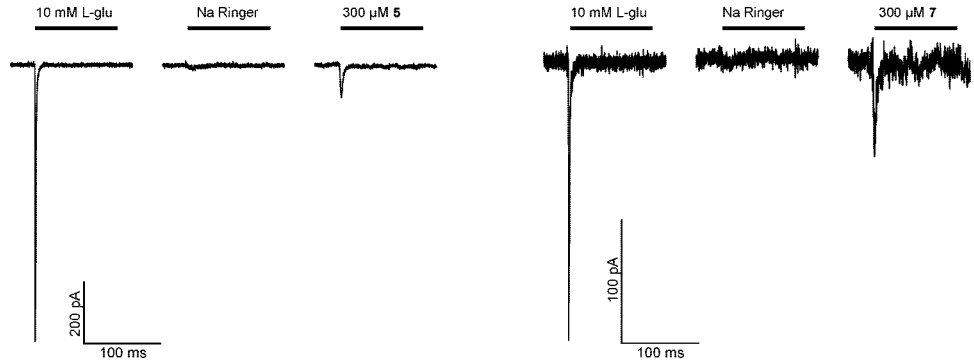

Figure 2. Representative current responses induced by **5** (left) or **7** (right) in iGluR5(Q)$_{1b}$ expressing cells, which were voltage-clamped at −60 mV in the whole-cell configuration. The cells were initially subjected to 100 ms pulses of 10 mM L-Glu. After the washout of Glu (NaRinger), a 100 ms pulse of **5** or **7** was applied to the cell.

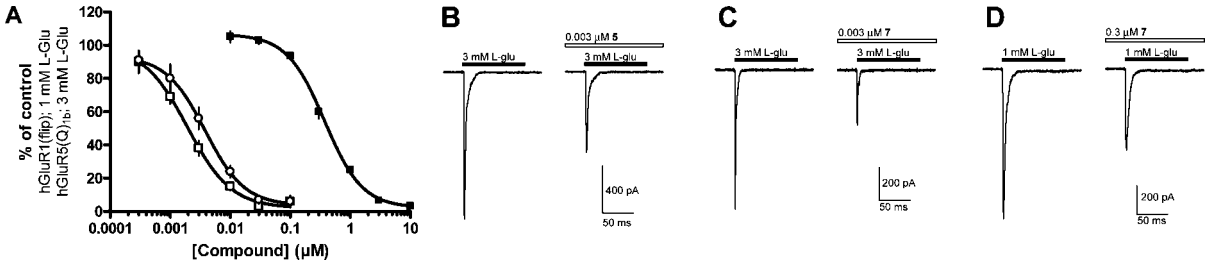

Figure 3. Compounds **5** and **7** desensitize both human iGluR1$_i$ and iGluR5(Q)$_{1b}$ receptors expressed in CHO-K1 cells. (A) Dose−response curve for the inactivation of iGluR5(Q)$_{1b}$ by **5** (open circles, IC_{50} = 3.8 nM) and **7** (open squares, IC_{50} = 1.9 nM) and of iGluR1$_i$ by **7** (filled squares, IC_{50} = 374 nM). The cells were stimulated with 100 ms control pulses of 3 mM L-Glu (iGluR5(Q)$_{1b}$) or 1 mM L-Glu (iGluR1$_i$) in 30 s intervals. When a stable response level was obtained, the cells were pretreated with **5** and **7**, before the next pulses with L-Glu. Values were normalized to the control L-Glu currents in the absence of **5** or **7** and represent the mean ± SEM of 4−10 separate experiments. (B) Representative L-Glu (3 mM) induced current responses at iGluR5(Q)$_{1b}$ receptors without (left) and in the presence of 3 nM **5** (right). (C) Representative L-Glu (3 mM) induced current responses at iGluR5(Q)$_{1b}$ receptors without (left) and in the presence of 3 nM **7** (right). (D) Representative L-Glu (1 mM) induced current responses at iGluR1$_i$ receptors without (left) and in the presence of 300 nM **7** (right).

better understanding of the different roles and modes of action of iGluR1−6 subunits, paving the way for the synthesis of new potent, subunit selective iGluR5 modulators.

Experimental Procedures

The synthesis of **3**−**11** was performed according to Schemes 1−5 in Supporting Information. We describe herein the synthesis of the most representative analogues of the series.

(*R*)-1-(2-Amino-2-carboxyethyl)-6,7-dihydro-1*H*-cyclopenta[*d*]-pyrimidin-2,4(1*H*,3*H*)dione (1). 1 was prepared starting from (*R*)-3-[*tert*-(butoxycarbonyl)amino]oxetan-2-one following the procedure previously reported for (*S*)-**1**.[4] Analytical data were identical to those reported for (*S*)-**1**.[4]

(*S*)-1-(3′-Amino-3′-carboxypropyl)-6,7-dihydro-1*H*-cyclopenta[*d*]-pyrimidin-2,4(3*H*,5*H*)-dione (3). To a solution of **14** (110.0 mg, 0.23 mmol) in methanol (10.0 mL) a catalytic amount of 10% Pd/C was added. The suspension was shaken for 8 h at room temperature in a Parr hydrogenator under 40 psi of H_2. Then the mixture was filtered through Celite and washed with methanol. The filtrate was concentrated, and the resulting crude product was purified by means of ion exchange chromatography (Dowex 50 WX 8-400 purchased from Aldrich), using first a mixture water/ethanol 1:1 v/v as eluent and after pyridine 1 M in water to recover the pure compound from the resin. Compound **3** was obtained as a colorless oil in 92.0% yield. ^{1}H NMR (200 MHz, D_2O/DCl 20 wt % in D_2O 9:1) δ 3.83−3.69 (m, 3H), 2.43 (m, 2H), 2.23 (m, 2H), 1.95 (m, 2H), 1.71 (m, 2H); ^{13}C NMR (300 MHz D_2O/DCI 20 wt % in D_2O 9:1) δ 170.2, 164.3, 157.6, 153.8, 111.6, 50.1, 36.6, 31.2, 30.4, 27.7, 26.7; ESI-MS *m/z* 252 (M − H)$^-$; $[\alpha]_D^{20}$ −21.0 (*c* 0.3, HCl 6N). Anal. ($C_{11}H_{15}N_3O_4$) C, H, N.

(*S*,*S*)-1,3-Di(3′-amino-3′-carboxypropyl)-6,7-dihydro-1*H*-cyclopenta[*d*]pyrimidin-2,4(3*H*,5*H*)-dione (4). 4 was obtained from **15** (1.13 g, 1.41 mmol) following the procedure described for **3** but increasing the pressure of H_2 (90 psi) and the reaction time (4 days). Compound **4** was obtained as an amorphous solid in 82.1% yield. ^{1}H NMR (200 MHz, D_2O/DCl 20 wt % in D_2O 9:1) δ 3.13 (m, 2H), 2.87 (m, 4H), 1.80 (t, 2H, *J* = 7.3 Hz), 1.44 (t, 2H, *J* = 7.6 Hz), 1.15 (m, 4H), 0.88 (m, 2H); ESI-MS *m/z* 353 (M − H)$^-$; $[\alpha]_D^{20}$ −7.4 (*c* 0.3, HCl 1 N). Anal. ($C_{15}H_{22}N_4O_6$) C, H, N.

(*S*)-1-[2′-Amino-2′-carboxyethyl]-5,7-dihydrothieno[3,4-*d*]pyrimidin-2,4(1*H*,3*H*)-dione (5). A mixture of **19a** (0.70 g, 1.96 mmol) in dichloromethane (5.0 mL) and trifluoroacetic acid (5.0 mL) was stirred for 16 h at room temperature. Then the solvent was removed and the crude product was purified by means of ion-exchange resin as described for derivative **3**. Compound **5** was obtained as a white amorphous solid in 74.8% yield. ^{1}H NMR (200 MHz, CD_3OD/DCl 20 wt % in D_2O 9:1) δ 4.51 (m, 1H), 4.35 (m, 4H), 3.92 (t, 2H, *J* = 3.1 Hz); ^{13}C NMR (300 MHz, D_2O/DCI 20 wt % in D_2O 9:1) δ 169.4, 162.5, 155.0, 153.6, 113.0, 52.4, 45.9, 36.0, 32.1; ESI-MS *m/z* 513 (100) (2M − H)$^-$, 256 (M − H)$^-$; $[\alpha]_D^{20}$ −14.1 (*c* 0.2, HCl 1 N). Anal. ($C_9H_{11}N_3O_4S$) C, H, N.

(*S*)-1-(2′-Amino-2′-carboxyethyl)-6,6-dimethyl-2,3,4,5,6,7-hexahydrocyclopentapyrimidin-2,4-dione (6). 6 was synthesized, starting from **19b**, following the synthetic strategy reported for **5**. Compound **6** was obtained as a white amorphous solid in 64% yield. ^{1}H NMR (200 MHz, D_2O/DCl 20 wt % in D_2O 9:1) δ 4.33−4.24 (m, 1H), 4.16−4.11 (m, 2H), 2.62 (s, 2H), 2.28 (s, 2H), 0.98 (s, 6H); ^{13}C NMR (300 MHz, D_2O/DCI 20 wt % in D_2O 9:1) δ 168.2, 163.5, 158.2, 153.2, 111.7, 51.4, 45.4, 44.8, 40.6, 37.1, 27.8; ESI-MS *m/z* 266 (M − H)$^-$; $[\alpha]_D^{20}$ −46 (*c* 0.5, HCl 1 N). Anal. ($C_{12}H_{17}N_3O_4$) C, H, N.

(*S*)-1-(2′-Amino-2′-carboxyethyl)thieno[3,2-*d*]pyrimidin-2,4-dione (7). 7 was synthesized, starting from **21**, following the synthetic strategy reported for **5**. Compound **7** was obtained as an amorphous solid in 10.0% yield. ^{1}H NMR (200 MHz, CD_3OD/DCl 20 wt % in D_2O 9:1) δ 8.09 (d, 1H, $J = 5.5$ Hz), 7.30 (d, 1H, $J = 5.5$ Hz), 4.61 (m, 2H), 4.45 (m, 1H); ^{13}C NMR (300 MHz, D_2O/DCl 20 wt % in D_2O 9:1) δ 169.6, 160.5, 153.3, 147.4, 138.1, 116.9, 113.5, 52.4, 45.4; ESI-MS *m*/*z* 509 (100) $(2M - H)^-$, 254 $(M - H)^-$, 167; $[\alpha]_D^{20}$ −9.7 (*c* 0.2, HCl 1 N). Anal. ($C_9H_9N_3O_4S$) C, H, N.

(*S*)-1-(2′-Amino-2′-carboxyethyl)quinazoline-2,4(1*H*,3*H*)-dione (8). Derivative **24** (75.0 mg, 0.17 mmol) and a catalytic amount of Pd/C 10% were added to solution of ammonium formate (20.0 mL, 0.4 N) in dry methanol. The mixture was heated to reflux and stirred for 24 h. Then the mixture was filtered through Celite and the filtrate evaporated under vacuum to give a white solid that was used in the next step without further purification. Deprotection of the amino function as described for **5** afforded **8** as an amorphous solid (98.7% yield). ^{1}H NMR (200 MHz, D_2O/DCl 20 wt % in D_2O 9:1) δ 7.70 (m, 1H), 7.47 (m, 1H), 7.04 (m, 2H), 4.34 (m, 2H), 4.26 (m, 1H); ^{13}C NMR (300 MHz, D_2O/DCI 20 wt % in D_2O 9:1) δ 168.9, 164.0, 152.0, 139.8, 136.7, 130.5, 128.2, 124.3, 115.430, 51.3, 42.2; ESI-MS *m*/*z* 250 $(M + H)^+$; $[\alpha]_D^{20}$ +14.8 (*c* 0.3, HCl 1 N). Anal. ($C_{11}H_{11}N_3O_4$) C, H, N.

(*S*)-1-(2′-Amino-2′-carboxyethyl)-3-benzylquinazoline-2,4(1*H*,3*H*)-dione (9). 9 was obtained, starting from **24**, following the synthetic strategy used for **5**. Compound **9** was obtained as a white amorphous solid in 95.6% yield. ^{1}H NMR (200 MHz, DMSO-d_6) δ 8.03 (d, 1H, $J = 7.8$ Hz), 7.76 (m, 1H), 7.53 (d, 1H, $J = 8.6$ Hz), 7.33−7.17 (m, 6H), 5.06 (s, 2H), 4.55 (m, 2H), 4.14 (t, 1H, $J = 7.1$ Hz); ^{13}C NMR (300 MHz, DMSO-d_6) δ 174.6, 168.9, 151.7, 142.9, 139.9, 137.3, 136.5, 129.0 (2C), 128.1, 115.8, 114.9, 98.6, 50.0, 45.1 43.1; ESI-MS *m*/*z* 340 $(M + H)^+$; $[\alpha]_D^{20}$ +55.7 (*c* 0.3, HCl 1 N). Anal. ($C_{18}H_{17}N_3O_4$) C, H, N.

(*S*)-1-(2′-Amino-2′-carboxyethyl)-3-benzylfuro[3,4-*d*]pyrimidin-2,4-dione (10). The title compound was obtained, starting from **28a**, following the synthetic strategy used for **5**. Compound **10** was obtained as a white amorphous solid in 87.5% yield. ^{1}H NMR (200 MHz, D_2O/DCl 20 wt % in D_2O 9:1) δ 7.61 (s, 1H), 7.10 (s, 1H), 6.65 (m, 5H), 4.41 (s, 2H), 3.90 (m, 1H), 3.72 (m, 2H); ESI-MS *m*/*z* 328 $(M - H)^-$, 284, 241; $[\alpha]_D^{20}$ +31.0 (*c* 0.2, HCl 1 N). Anal. ($C_{16}H_{15}N_3O_5$) C, H, N.

(*S*)-1-(2′-Amino-2′-carboxyethyl)furo[3,4-*d*]pyrimidin-2,4-dione (11). 11 was obtained, starting from **28b**, following the same synthetic strategy used for **5**. Compound **11** was obtained as a white amorphous solid in 95% yield. ^{1}H NMR (200 MHz, D_2O/DCl 20 wt % in D_2O 9:1) δ 8.07 (s, 1H), 7.55 (s, 1H), 4.37−4.31 (m, 1H), 4.25−4.19 (m, 2H); ESI-MS *m*/*z* 240 $(M + H)^+$, 223, 194; $[\alpha]_D^{20}$ +38.0 (*c* 0.5, HCl 1 N). Anal. ($C_9H_9N_3O_5$) C, H, N.

Acknowledgment. This work was partially supported by the MIUR-PRIN, the Novo Nordisk Foundation, and the Danish Medical Research Council. The authors thank NeuroSearch A/S Ballerup, Denmark.

Supporting Information Available: Chemistry, Schemes 1−5, experimental procedures for intermediates, elemental analysis results for final compounds. This material is available free of charge via the Internet at http://pubs.acs.org.

References

(1) Bräuner-Osborne, H.; Egebjerg, J.; Nielsen, E.; Madsen, U.; Krogsgaard-Larsen, P. Ligands for glutamate receptors: design and therapeutic prospects. *J. Med. Chem.* **2000**, *43*, 2609–2645.

(2) (a) Rosenmund, C.; Stern-Bach, Y.; Stevens, C. F. The tetrameric structure of a glutamate receptor channel. *Science* **1998**, *280*, 1596–1599. (b) Sun, Y.; Olson, R.; Horning, M.; Armstrong, N.; Mayer, M.; Gouaux, E. Mechanism of glutamate receptor desensitization. *Nature* **2002**, *417*, 245–253. (c) Laube, B.; Kuhse, J.; Betz, H. J. Evidence for a tetrameric structure of recombinant NMDA receptors. *Neuroscience* **1998**, *18*, 2954–2961.

(3) Frandsen, A.; Schousboe, A. Excitatory amino acid-mediated cytotoxicity and calcium homeostasis in cultured neurons. *J. Neurochem.* **1993**, *60*, 1202–1211.

(4) Campiani, G.; Morelli, E.; Nacci, V.; Fattorusso, C.; Ramunno, A.; Novellino, E.; Greenwood, J.; Liljefors, T.; Griffiths, R.; Sinclair, C.; Reavy, H.; Kristensen, A. S.; Pickering, D. S.; Schousboe, A.; Cagnotto, A.; Fumagalli, E.; Mennini, T. Characterization of the 1*H*-cyclopentapyrimidine-2,4(1*H*,3*H*)-dione derivative (*S*)-CPW399 as a novel, potent, and subtype-selective AMPA receptor full agonist with partial desensitization properties. *J. Med. Chem.* **2001**, *44*, 4501–4504.

(5) Dolman, N. P.; Troop, H. M.; More, J. C. A.; Alt, A.; Knauss, J. L.; Nistico, R.; Jack, S.; Morley, R. M.; Bortolotto, Z. A.; Roberts, P. J.; Bleakman, D.; Collingridge, G. L.; Jane, D. E. Synthesis and pharmacology of willardiine derivatives acting as antagonists of kainate receptors. *J. Med. Chem.* **2005**, *48*, 7867–7881.

(6) Hogner, A.; Kastrup, J. S.; Jin, R.; Liljefors, T.; Mayer, M. L.; Egebjerg, J.; Larsen, I. K.; Gouaux, E. Structural basis for AMPA receptor activation and ligand selectivity: crystal structures of five agonist complexes with the GluR2 ligand-binding core. *J. Mol. Biol.* **2002**, *322*, 93–109.

(7) Mayer, M. L. Crystal structures of the GluR5 and GluR6 ligand binding cores: molecular mechanisms underlying kainate receptor selectivity. *Neuron* **2005**, *45*, 539–552.

(8) Frandsen, A.; Pickering, D. S.; Vestergaard, B.; Kasper, C.; Bryde Nielsen, B.; Greenwood, J. R.; Campiani, G.; Fattorusso, C.; Gajhede, M.; Schousboe, A.; Kastrup, J. S. Tyr702 is an important determinant of agonist binding and domain closure of the ligand-binding core of GluR2. *Mol. Pharmacol.* **2005**, *67*, 1–11.

(9) Dolman, N. P.; More, J. C. A.; Alt, A.; Knauss, J. L.; Pentikäinen, O. T.; Glasser, C. R.; Bleakman, D.; Mayer, M. L.; Collingridge, G. L.; Jane, D. E. Synthesis and pharmacological characterization of N^3-substituted willardiine derivatives: role of the substituent at the 5-position of the uracil ring in the development of highly potent and selective Glu_{K5} kainate receptor antagonists. *J. Med. Chem.* **2007**, *50*, 1558–1570.

(10) Kizelsztein, P.; Eisenstein, M.; Strutz, N.; Hollmann, M.; Teichberg, V. I. Mutant cycle analysis of the active and desensitized states of an AMPA receptor induced by willardiines. *Biochemistry* **2000**, *39*, 12819–12827.

(11) Greenwood, J. R.; Mewett, K. N.; Allan, R. D.; Martín, B. O.; Pickering, D. S. 3-Hydroxypyridazine 1-oxides as carboxylate bioisosteres: a new series of subtype-selective AMPA receptor agonists. *Neuropharmacology* **2006**, *51*, 52–59.

JM800865A